
ORIGINAL ARTICLE

The Dosimetric Effects of Ignoring Small Non-bone High-density Regions Using the 5-Bulk-density Method for Photon Dose Calculation

AI Saito, JG Li, C Liu, KR Olivier, D Kahler, K Karasawa, JF Dempsey

Department of Radiation Oncology, College of Medicine, University of Florida, Gainesville, FL, USA

ABSTRACT

Objective: To investigate the effect of the 5-bulk-density dose calculation method without considering small non-bone high-density regions in patients with thoracic cancers.

Methods: A heterogeneity-corrected computed tomography plan and two types of 5-bulk-density treatment plans were generated for patients with lung or oesophageal tumours without any obvious findings of emphysema. In the first 5-bulk-density plan, the bone was contoured using an auto-contouring tool; in the second plan, the bone was contoured manually ignoring small non-bone high-density regions. Treatment plans were made with a commercial treatment-planning system and an adaptive convolution dose-calculation algorithm. The population's average density was applied, and the heterogeneity-corrected plan was compared with all of the 5-bulk-density regions for each case. Dose-volume histograms and dose-difference distributions were examined for all cases.

Results: A total of 53 patients (57 tumours) were enrolled. Both the auto- and manually contoured plans had average bone and tissue densities of 1.12 g/cm³ and 1.02 g/cm³, respectively. When the manually contoured plan was compared with the heterogeneity-corrected plan, dose-volume histograms of the normal tissue and planning target volume agreed to within 2% of the dose.

Conclusions: For bulk-tissue-density heterogeneous dose calculation, clinically acceptable dosimetric accuracy was achieved for auto-contoured bone cases without considering small non-bone high-density regions. This means that the current method could be applied with magnetic resonance imaging in the treatment planning system for dose calculation where no electron density information exists.

Key Words: Bone density; Electrons; Lung neoplasms; Radiotherapy planning, computer-assisted; Radiotherapy, intensity-modulated

中文摘要

忽略微小的非骨性高密度區運用5倍體積密度法對光子劑量測定的效果

AI Saito, JG Li, C Liu, KR Olivier, D Kahler, K Karasawa, JF Dempsey

目的：探討忽略胸廓內腫瘤患者微小的非骨性高密度區的情況下，5倍體積密度的劑量計算方法的效果。

方法：替沒有任何明顯肺氣腫的肺腫瘤或食管腫瘤患者，制定組織異質性校正的電腦斷層掃描方案和兩種5倍體積密度治療方案。第一種5倍體積密度方案中，用自動工具勾劃出骨輪廓；第二種方案

Correspondence: Dr Ameyuko I Saito, 2-1-1, Tomioka, Urayasu-shi, Chiba 279-0021, Japan.
Tel: (81) 473533111; Fax: (81) 473533111; Email: anyusaike@yahoo.co.jp

Submitted: 22 Mar 2013; Accepted: 12 Aug 2013.

中，忽略微小的非骨性高密度區而人工勾劃出骨輪廓。運用商用治療規劃系統和自適應卷積劑量計算法來制定治療方案。利用人均密度，將每個病例的異質性校正方案與5倍體積密度方法的全部區域作比較；並檢視所有病例的劑量體積直方圖和劑量差異分佈。

結果：總計53名病人（共57個腫瘤）納入研究。自動和人工勾劃輪廓方案的平均骨骼和組織密度分別為1.12 g/cm³和1.02 g/cm³。人工勾劃輪廓方案與異質性校正方案相比，正常組織的劑量體積直方圖和靶區體積的差異均在2%以內。

結論：在異質性組織中運用體積-組織-密度劑量計算法，忽略微小的非骨性高密度區而採用骨輪廓自動勾劃法也能達至臨床可接受的劑量測定精確度。這意味着在治療規劃系統中，可運用該方法以無電子密度信息的磁共振圖像為基礎作劑量測定。

INTRODUCTION

We have reported that radiotherapy treatment planning using heterogeneity corrections for 5-bulk densities can be used in place of heterogeneity-corrected computed tomography (CT) treatment planning even in the thoracic area.¹ The application utilises an on-board image-guided radiation therapy (IGRT) device that is under development.² This IGRT device will utilise magnetic resonance imaging (MRI) in real time (taken during radiation delivery) to compute the dose delivered to the patient. Whereas segmented MRI studies can be used to identify bulk-density regions of air, lung, fat, soft tissue, and bone in a patient; the non-bone high-density regions of CT images are not easily identified with this technique. Instead of using CT-based treatment planning for the thoracic area, the 5-bulk-density method can be used without electron-density information. However, if an MRI is used for treatment planning,³⁻⁷ small calcified regions, such as those in the aortic wall, are impossible to identify. This common condition is found in many patients undergoing CT simulation for radiation therapy.

In our previous study,¹ we created a bone-density region using an auto-contouring tool for which we established a threshold density and then automatically contoured all of the structures that had a higher CT number than the threshold of 1080 HU. These structures included small calcifications, artefacts caused by high-density lesions, and higher-density areas in the soft tissue that could not be visualised when an MRI was used for treatment planning. The CT number of the Pinnacle³ treatment planning system (Philips Medical Systems, Andover [MA], USA), which we used for this and the previous study, is equal to 0 for air density.

The purpose of this study was to investigate whether the results of the 5-bulk-density dose calculation were

significantly affected by these small non-bone high-density areas, which would be ignored when the contouring was done manually.

METHODS

This study analysed anonymised CT planning image studies for lung and oesophageal cancers demonstrating gross tumour volumes treated at the University of Florida, Gainesville [FL], USA. These patients were the same as in our previous study.¹

All patients had undergone helical CT scans (Professional Series P220F; Philips Medical Systems, Eindhoven, The Netherlands) without contrast enhancement and with an axial-plane image-matrix size of 512 x 512, an in-plane pixel size of 1.1 mm, and a slice thickness of 3.0 mm covering the entire thorax and the superior portion of the abdomen. No intravenous contrast enhancement was used. However, to enhance the image, one patient with oesophageal cancer was administered barium sulphate cream (Esophocat 3.0%; E-Z-EM Canada Inc, Montreal, Canada). While in a sitting position on the CT simulation table, the patient swallowed one teaspoon of the contrast material then, while lying on the table, the patient swallowed half a teaspoon immediately before the scan was taken.

Heterogeneity-corrected CT resolution and bulk-electron-density treatment plans were generated for the patients using a commercial treatment planning system with an adaptive convolution dose-calculation algorithm (Pinnacle³) and employing an isotropic 4-mm dose-calculation grid. For each patient, bulk-electron densities were applied to regions identified by an isodensity segmentation tool. The word ‘density’ is used to indicate electron density relative to that of water.

The precise methodology of 5-bulk-density segmentation

is described elsewhere.¹ In brief, the trachea, lung, fat, and bone were contoured and the soft-tissue-density region was generated by subtracting these contours from the body contour. The population-average data of 66 patients determined the electron density for each region; the densities assigned to air, lung, fat, soft tissue, and bone were 0.14, 0.26, 0.89, 1.02, and 1.12 g/cm³, respectively. For patients with specific pathological conditions such as bullous formations, pneumothorax or hiatus hernia, the density of air was assigned to the pathological regions.

For each patient, three plans were created: (1) a heterogeneity-corrected CT plan that was referred to as the original plan (Figure 1a); (2) an auto-contoured bone plan, for which the bone was contoured automatically using the threshold 1080-4500 HU using the 5-bulk densities (Figure 1b); and (3) a manually contoured bone plan, for which the bone was contoured manually using the 5-bulk densities (Figure 1c). Implantable port reservoirs were contoured for the bones, but calcifications, CT artefacts, high-density areas in the soft tissue, and oral contrast media for the gastrointestinal tract were excluded. All plans were simple, with two opposed 10-MV beams (at 0° and 180°) and no intensity-modulated radiation therapy (IMRT) or stereotactic body radiotherapy was employed. The weighting was the same for both beams. Original monitor units were used for all three plans, and no normalisations or adjustments were made.

Dose-volume histogram (DVH) and slice-by-slice comparisons of dosimetry for the treatment area were performed for all plans. We specifically investigated the following parameters: the dose covering 95% or more (D95) of the planning target volume (PTV); the mean PTV dose; the percentage of the total lung volume receiving 20 Gy or higher (V20Gy %); and the mean total lung dose. If the dose or volume differences were within 2% of the original plan, the plan was regarded as acceptable. For the slice-by-slice comparisons, we calculated the percentage of dose-grid voxels that showed more than 5% disagreement in the area with less than 3% of the maximum dose gradient.

RESULTS

Fifty-three patients with 57 tumours were enrolled in the study. Table 1 shows the patients' demographics. All patients who attended the Department of Radiation Oncology for thoracic radiotherapy were included except for those who underwent IMRT or stereotactic

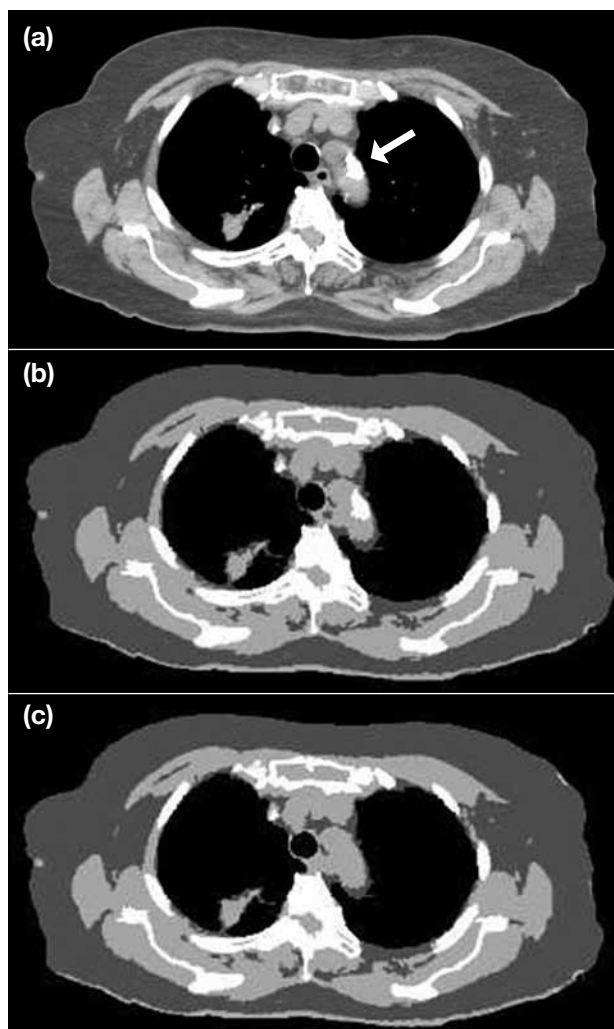


Figure 1. Computed tomography images used for creating the three plans. (a) Original heterogeneity-corrected image (original), calcification of the aorta (arrow) is observed; (b) image created using the 5-bulk densities, the bones are contoured automatically by using the threshold 1080-4500 HU (auto-contoured); and (c) image created using the 5-bulk densities, the bones are contoured manually (manual).

body radiotherapy. Tables 2 and 3 summarise the mean and percentage differences in dose volume between the three plans. In general, no significant differences were observed for either the PTV or critical-structure doses. For the critical structures, which included the lung, heart and spinal cord, no differences greater than 2% in either dose or volume were observed in any of the DVHs. Figure 2 shows a DVH for a typical patient, with good agreement between the plans (the DVH of the three plans are displayed as an overlay). There were no differences greater than 2% between the original and manual plans (the largest difference observed was 1.85% in the mean PTV dose). Moreover, there were no differences greater than 1% between the auto-contoured

Table 1. Patient characteristics.

Characteristic	No. of patients
Sex	
Female	17
Male	36
Race	52
Black	4
White	49
Median (range) age (years)	66 (17-88)
Median (range) body mass index (kg/m ²)	25 (13-53)
Tumour site	
Oesophagus	13
Lung	40
Lung tumour position	
Left lobe	22
Mediastinum and / or hilum	7
Right lobe	15
Upper lung field	28
Middle lung field	13
Lower lung field	3
Oesophagus tumour position	
Middle oesophagus	2
Inferior oesophagus	11
Lung and gastrointestinal tract conditions in the treatment area	
Bullous formation	6
Pneumothorax	2
Hiatus hernia	1
Median (range) total dose (Gy)	4500 (2000-6300)
Energy (MV)	
6	42
>6	11
Median (range) No. of beams	4 (2-8)

and manual plans (the largest difference observed was 0.62% in D95 of the PTV).

In addition, in the slice-by-slice comparisons of

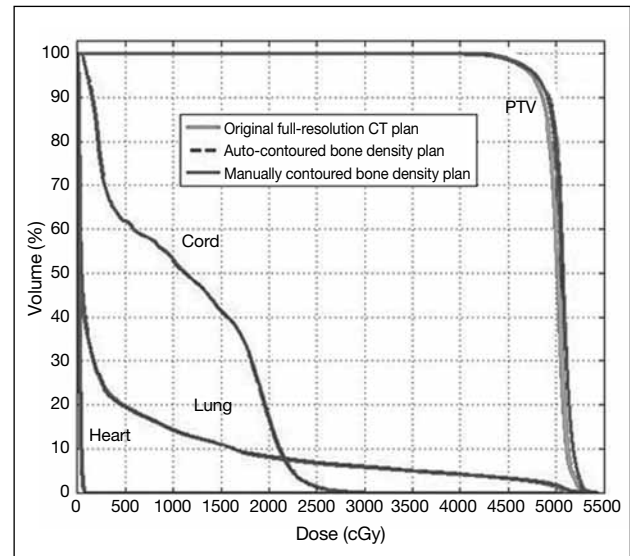


Figure 2. Typical dose-volume histogram of the planning target volume and cord, lung, and heart of the three plans. The auto-contoured bone density plan is (dotted line) is almost the same as the manually contoured bone density plan.

Abbreviations: CT = computed tomography; PTV = planning target volume.

Table 2. Dosimetric comparison between original heterogeneity-corrected computed tomography plans (original), 5-bulk-density plans in which the bones are automatically contoured (auto-contoured), and 5-bulk-density plans in which the bones are manually contoured (manual).

	Original		Auto-contoured		Manual	
	Mean	SD	Mean	SD	Mean	SD
PTV D95* (cGy)	3898	1274	3928	1284	3928	1284
PTV mean dose (cGy)	4134	1178	4162	1186	4162	1186
Lung V20Gy† (%)	12.82	7.95	13.00	7.88	13.01	7.89
Lung mean dose (cGy)	731	389	738	396	738	396

Abbreviations: PTV = planning target volume; SD = standard deviation.

* PTV D95 represents the dose covering ≥95% of the PTV.

† Lung V20Gy represents the percentage of lung volume covered by ≥20 Gy.

Table 3. Differences (in Gy) of D95, mean dose of PTV, and V20Gy, and mean dose to lung between original heterogeneity-corrected computed tomography plans (original), 5-bulk-density plans in which the bones are automatically contoured (auto-contoured), and 5-bulk-density plans in which the bones are manually contoured (manual).

	Original vs. manual			Auto-contoured vs. manual		
	Mean	SD	No.*	Mean	SD	No.*
PTV D95† (%)	0.79	0.49	0	0.05	0.1	0
PTV mean dose (%)	0.77	0.46	0	0.03	0.04	0
Lung V20Gy† (%)	0.28	0.46	0	0.02	0.08	0
Lung mean dose (%)	0.24	0.18	0	<0.01	0.01	0

Abbreviations: PTV = planning target volume; SD = standard deviation.

* No. of tumours where the difference was ≥2%.

† PTV D95 represents the dose covering ≥95% of the PTV.

‡ Lung V20Gy represents the percentage of lung volume covered by ≥20 Gy.

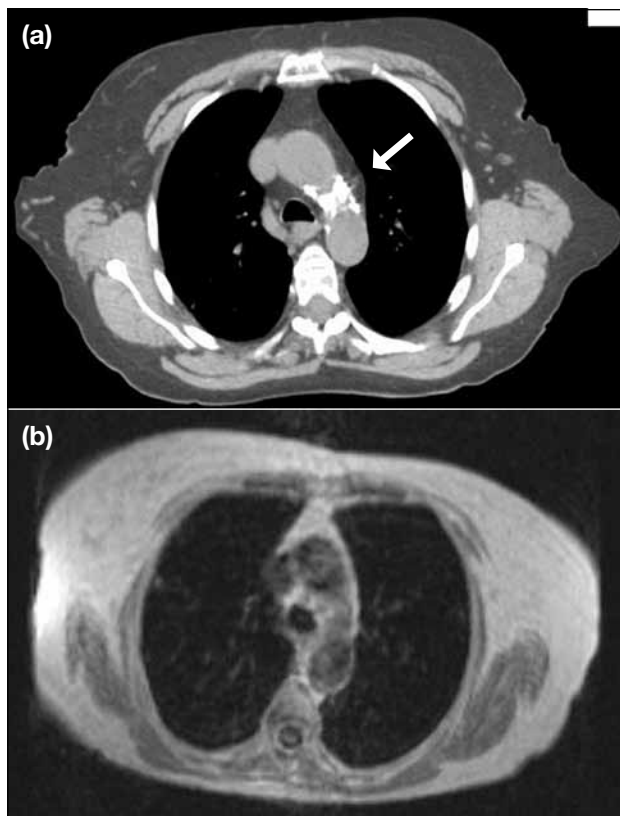


Figure 3. Images of a patient with calcification of the aorta (arrow). (a) Computed tomography (CT) image; and (b) magnetic resonance image (0.2 T, T1-weighted) of a slice similar to the CT image.

dosimetry for the treatment areas (for both the original vs manual and the auto-contoured vs. manual plans), no cases showed >1% of the voxels with >5% of dose difference in a low-gradient region (original vs. manual mean, 0.18%; standard deviation [SD], 0.23%; auto-contoured vs. manual mean, 0.10%; SD, 0.19%).

DISCUSSION

The 5-bulk-density dose calculation method¹ eliminates the need for electron-density information, even for the thoracic area. However, some issues arise when the method is used for MRI treatment planning. MRI is less sensitive to calcification than CT; thus, CT imaging can identify small calcifications such as those of the large vessels (Figures 1a, 1b, and 3), and high-density regions such as the thyroid gland that MRI cannot identify. Furthermore, MRI is unable to detect CT-identifiable, non-calcified, high-density areas, such as soft tissue in the superior region of the thorax (Figure 4) or contrast in the oesophagus (Figure 5).

Patients who repeatedly receive chemotherapy sometimes have an implantable port reservoir inserted.

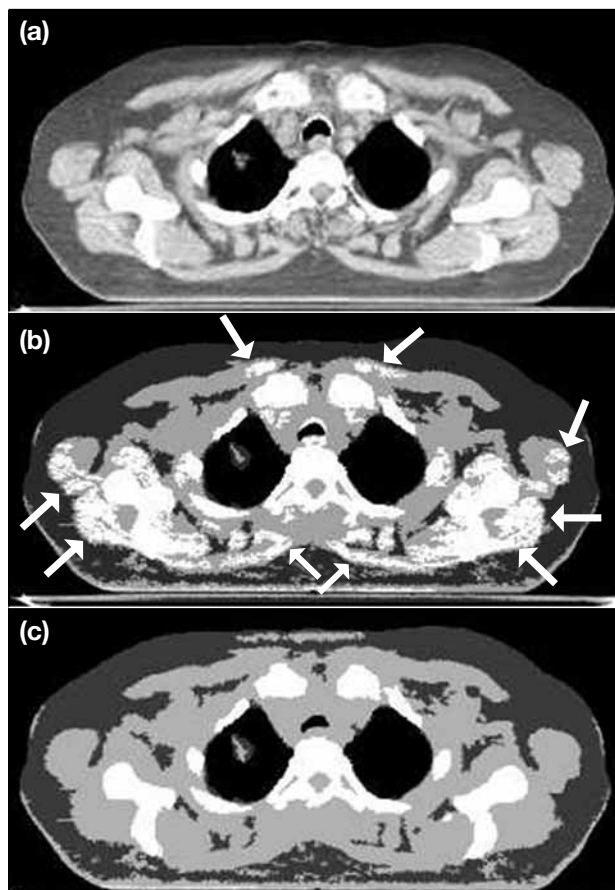


Figure 4. Computed tomography images of a patient with high-density areas in the upper thoracic soft-tissue area. Even when treating the tumour at the right apex, the dosimetric differences between the three plans are minimal. (a) Original heterogeneity-corrected image (original); (b) image created using the 5-bulk densities, the bones are contoured automatically by using the threshold 1080-4500 HU (auto-contoured) and because the densities of the muscles are high, they are defined as bone on this image (arrows); and (c) image created using the 5-bulk densities, the bones are contoured manually (manual).

An implantable port reservoir is easy to detect on both CT and MRI; therefore, we contoured them as 'bone' in the manual plan (Figure 6). However, the catheters connected to them, which contain high-density material, are easy to detect on CT, but not on MRI (Figures 7a and 7b). Also, there are CT-detectable artefacts caused by these kinds of high-density regions (Figure 7c) that are seen during treatment planning, but do not actually exist, as well as oral contrast-enhancement materials that disappear after treatment planning. In these situations, the manual plan is more accurate than the auto-contoured plan, since the auto-contoured plan may detect artefacts in high-density regions that do not exist during the treatment.

In our previous study, we used an automated method to

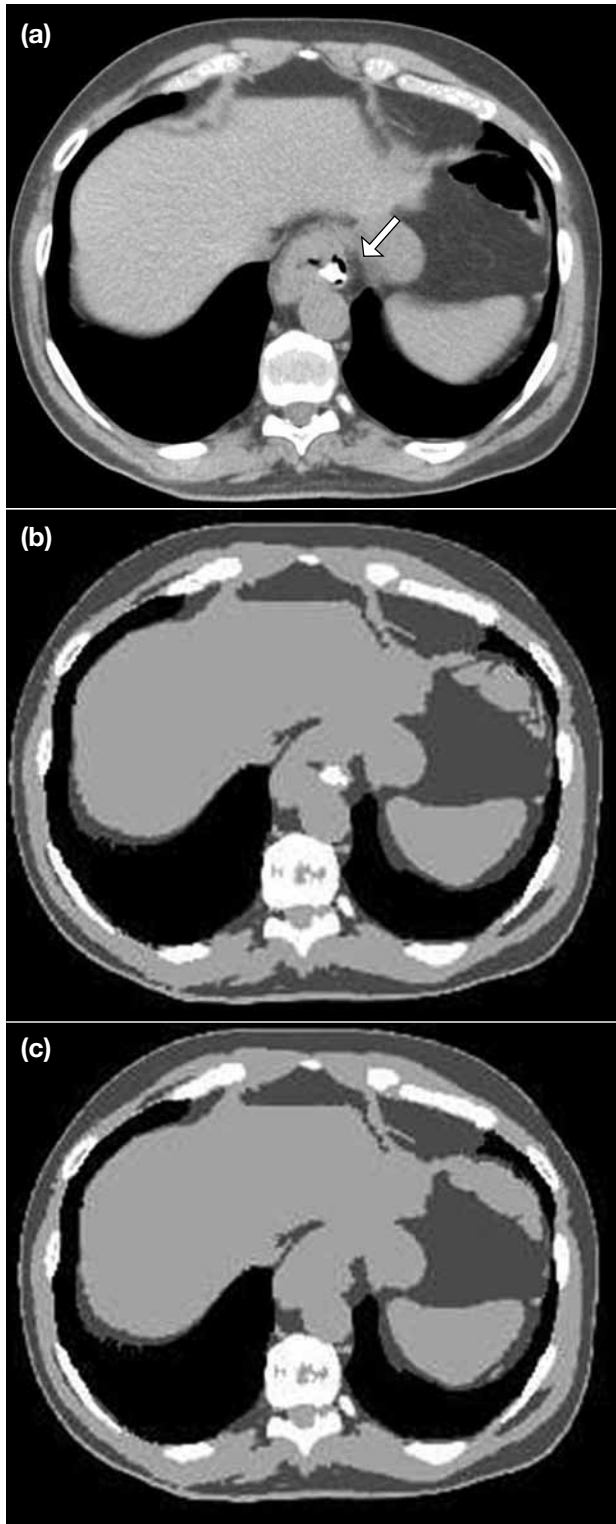


Figure 5. Original heterogeneity-corrected computed tomography images of a patient with oral contrast-enhancing material for detecting oesophageal cancer. (a) Original heterogeneity-corrected image (original), oral contrast-enhancing material is shown with an arrow; (b) image created using the 5-bulk densities, the bones are contoured automatically by using the threshold 1080-4500 HU (auto-contoured); and (c) image created using the 5-bulk densities, the bones are contoured manually (manual).

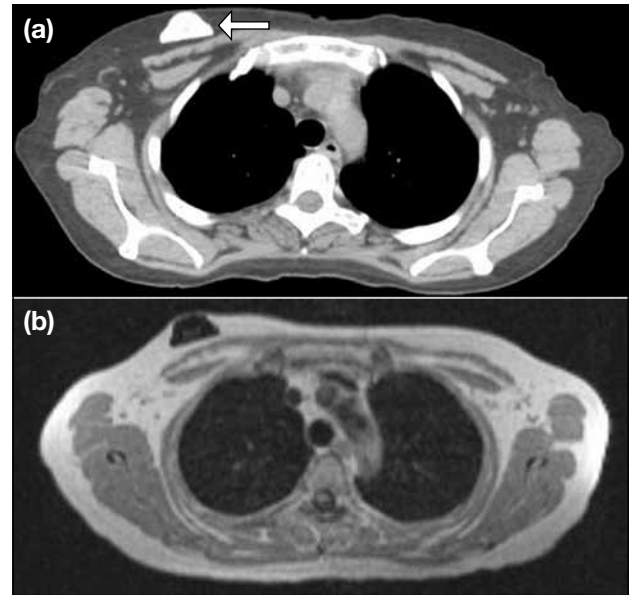


Figure 6. Images of a patient with a port reservoir (arrow). (a) Computed tomography (CT) image and (b) magnetic resonance image (0.2 T, T1-weighted) of a slice similar to the CT image.

contour bone.¹ With this method, the high-density areas above a certain threshold were included in the bone-density region. The purpose was to investigate whether or not the 5-bulk-density dose calculation method would be compromised if the MRI-detectable region was manually contoured and assigned as bone density. When we compared the manual with the original plan DVH, we found that there were no patients for whom a $\geq 2\%$ difference was seen in either dose or volume for either the PTV or critical organs. The difference between the manual and auto-contoured plans, with a maximum difference of 0.62% in D95, was even less. In the slice-by-slice comparisons for both the original versus manual and auto-contoured versus manual plans, no cases showed $>1\%$ of the voxels with a $>5\%$ difference in a low-gradient region (maximum, 0.96% and 0.77%, respectively). Of the 12 oesophageal cancer patients, 10 had contrast material in the PTV; nine patients had large calcifications in the PTV, and three patients had postoperative clips with strong artefacts; nevertheless, the effect of these conditions on the dosimetry was not significant.

Presently, even in the thoracic area of treatment and especially for stereotactic body radiotherapy, more than 2 beams are employed. However, only opposing beams of 10-MV photons with entry angles at 0° and 180° (same weighting) were studied. This is because the simple direct beams would be more affected by the

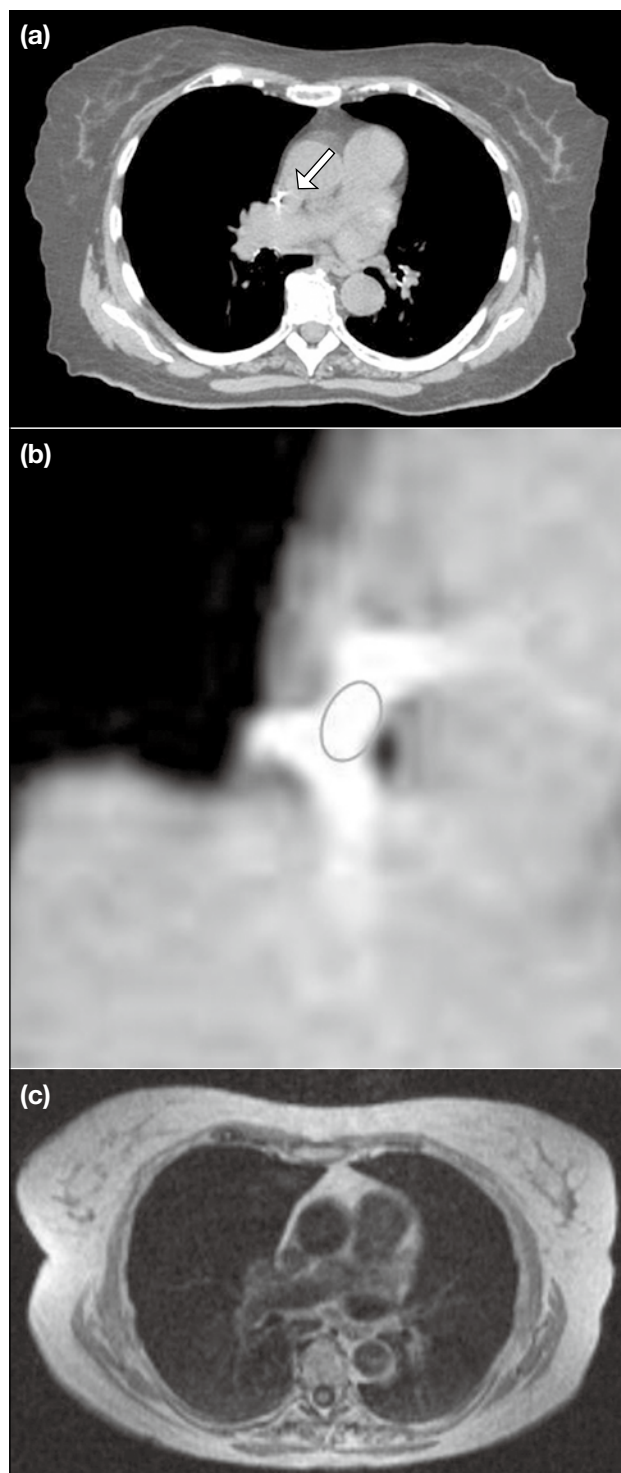


Figure 7. Images of a patient with a catheter connected to the port reservoir. (a) Computed tomography (CT) image of the catheter (arrow; because of the strong density of the catheter, artefacts are observed); (b) enlarged computed tomography image of the catheter (circle) with artefacts around it; and (c) magnetic resonance image (0.2 T, T1-weighted) of a slice similar to the CT image.

high-density areas. Had more complicated planning such as 3-dimensional, IMRT, or Volume Activation Management Tool been used, the beams entering from several directions and the modulated intensity would have offset the effect from the high-density area because the high-density areas exist only in restricted, relatively small, areas.

Even if the bones were manually contoured and the small calcifications and high-density areas in the body were assigned as soft-tissue density, the heterogeneity correction for 5-bulk densities could still be used for accurate radiotherapy treatment planning. Thus, this method could be employed for treatment planning using MRI, for which the sensitivity to calcification is lower than that for CT.

CONCLUSION

For treatment planning done with an IGRT device without electron-density information provisions, even if the small high-density regions are not detectable, bulk-tissue-density heterogeneous dose calculation can enable clinically acceptable dosimetric accuracy for auto-contoured bone without considering small non-bone high-density regions.

REFERENCES

1. Saito AI, Li JG, Liu C, Olivier KR, Dempsey JF. Accurate heterogeneous dose calculation for lung cancer patients without high-resolution CT densities. *J Appl Clin Med Phys.* 2009;10:2847.
2. Raaijmakers AJ, Raaymakers BW, Lagendijk JJ. Magnetic-field-induced dose effects in MR-guided radiotherapy systems: dependence on the magnetic field strength. *Phys Med Biol.* 2008;53:909-23. [crossref](#)
3. Khoo VS, Adams EJ, Saran F, Bedford JL, Perks JR, Warrington AP, et al. A comparison of clinical target volumes determined by CT and MRI for the radiotherapy planning of base of skull meningiomas. *Int J Radiat Oncol Biol Phys.* 2000;46:1309-17. [crossref](#)
4. Pötter R, Heil B, Schneider L, Lenzen H, al-Dandashi C, Schnepfer E. Sagittal and coronal planes from MRI for treatment planning in tumors of brain, head and neck: MRI assisted simulation. *Radiother Oncol.* 1992;23:127-30. [crossref](#)
5. Sannazzari GL, Ragona R, Ruo Redda MG, Giglioli FR, Isolato G, Guarneri A. CT-MRI image fusion for delineation of volumes in three-dimensional conformal radiation therapy in the treatment of localized prostate cancer. *Br J Radiol.* 2002;75:603-7.
6. Tanner SF, Finnigan DJ, Khoo VS, Mayles P, Dearnaley DP, Leach MO. Radiotherapy planning of the pelvis using distortion corrected MR images: the removal of system distortions. *Phys Med Biol.* 2000;45:2117-32. [crossref](#)
7. Chen L, Nguyen TB, Jones E, Chen Z, Luo W, Wang L, et al. Magnetic resonance-based treatment planning for prostate intensity-modulated radiotherapy: creation of digitally reconstructed radiographs. *Int J Radiat Oncol Biol Phys.* 2007;68:903-11. [crossref](#)